Flexure Toughness of Polymer Fiber-reinforced Cementitious Materials

VENKATA K. PUNYAMURTULA AND YU QIAO*
Department of Structural Engineering, University of California – San Diego, La Jolla, CA 92093-0085, USA

ABSTRACT: In this article, the toughening effect of polymer fibers in cementitious materials is analyzed through an energy method. When a crack front encounters a fiber array, additional fracture work is required to overcome the barrier effect. The influences of fibers, matrix, and crack length on the critical energy release rate are collectively described by a single system parameter.

KEY WORDS: fracture toughness, fiber, cement, composite.

INTRODUCTION

EACH YEAR, MORE than 10 billion tons of concretes were used. Although they are usually designed for compressive-load-carrying applications, tensile damages in brittle cementitious phases associated with drying creep, aging, thermal expansion, freezing and thawing, relaxation of pre-stresses, etc. are reported frequently (Mamlouk and Zniewski, 1999; Ulm, 2003; Zou 2003; Barbero et al., 2005). Therefore, it is immensely important to develop advanced reinforcing techniques. Over the years, fiber-reinforced cements (FRC) were studied intensively (e.g., Zollo, 1997; Bayasi and Al Dhaheri, 2002; Chan et al., 2005; Ju et al., 2006; Ouaar et al., 2007). With the addition of tough, well dispersed short fibers, the resistance to catastrophic cracking under tensile loadings can be considerably enhanced. Among many available materials such as steels and glasses, polymer fibers have received increasing attention (Mindess et al., 2002).

When a propagating crack front encounters a polymer fiber array, the homogenous growth will be disrupted as the front penetrates between the

*Author to whom correspondence should be addressed. E-mail: yqiao@ucsd.edu
Figure 1 appears in color online: http://ijd.sagepub.com

1056-7895/08/04 0363–9 $10.00/0 DOI: 10.1177/1056789508092398

fibers, and additional fracture work is required to overcome the barrier effect (Bayasi and McIntyre, 2002; Kodur et al., 2003; Banthia and Nandakumar, 2003). As the penetration depth increases, the bridging force rises rapidly and eventually the fibers will fail, either through fiber pull-out or breakage. Due to the decrease in fracture resistance, the crack front will jump forward until the crack growth driving force is reduced to the critical value to arrest the advancing crack. During this process, a certain amount of the strain energy stored in the sample is dissipated because of the increase in fracture surface area and the failure of fibers (Qiao, 2003).

A number of experimental studies have been carried out (Mower and Argon, 1995; Kamada and Li, 2000), and several numerical procedures have been developed to analyze the fracture resistance of reinforcing fibers (Kullaa, 1994; Lee et al., 1995; Haj Ali and El Hajjar, 2004). However, most of these studies were focused on the fiber-crack interaction at the verge of propagating front and shed little light on the fracture work distribution. In this work, we study the toughening effect of polymer fibers through an energy analysis. The overall toughening effect consists of the contributions from the barrier effect of the fibers at the crack tip and from the post-cracking bridging effect of the fibers exposed in the fracture surface. The important system parameters such as fiber aspect ratio and volume fraction are discussed in detail.

TOUGHENING EFFECTS OF A REGULAR FIBER ARRAY AT THE CRACK TIP

Tensile toughness of cementitious materials is usually evaluated through flexure performance measurement (ASTM C78). Figure 1(a) shows a standard four-point bending test of a cement beam pre-cracked along the median plane. Two concentrated forces, P, are applied at the third points. The distances between the two ends and the two concentrated forces are

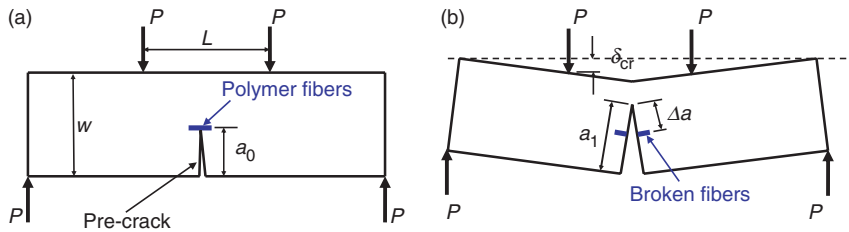

Figure 1. *Schematic of the four-point bending test of a cement beam reinforced by a regular fiber array: (a) prior to the crack jump; (b) immediately after the crack jump.*

the same. The length of the beam is equal to six times of the height. Assume that the beam is reinforced by a single regular fiber array at the pre-crack tip. The fibers are oriented parallel to the axial direction, i.e., they are perpendicular to the fracture surface. At rest the beam is subjected to a displacement-controlled force, P. The deflection rate, $\dot{\delta}$, is sufficiently low such that the loading process is quasi-static.

Prior to the crack propagation, as the deflection, δ, increases, P rises linearly. If the crack length, a, is below $0.7w$, the strain energy stored in the beam, U, can be obtained by integrating the energy release rate, G, with respect to the crack length, a (Gross and Srawley, 1972)

$$U = \frac{144(1-\nu^2)\pi}{E} g_0(\tilde{a}) P^2 \tag{1}$$

where E is the effective modulus of elasticity and ν is the Poisson's ratio, w is the beam height, $g_0(\tilde{a}) = \int f(\tilde{a}) \mathrm{d}\tilde{a}$, $f(\tilde{a}) = \tilde{a} \cdot f_0^2(\tilde{a})$, $f_0(\tilde{a}) = 1.12 - 1.39\tilde{a} + 7.3\tilde{a}^2 - 13.0\tilde{a}^3 + 14.0\tilde{a}^4$, and $\tilde{a} = a/w$. Note that U and P are defined as the strain energy per unit thickness and the load per unit thickness, respectively. As $a \to 0$, Equation (1) converges to the elasticity solution of a uncracked plate. Since $U = P \cdot \delta$, we have

$$P = \frac{E}{144(1-\nu^2)\pi} \frac{\delta}{g_0(\tilde{a})} \tag{2}$$

and

$$U = \frac{E}{144(1-\nu^2)\pi} \frac{\delta^2}{g_0(\tilde{a})}. \tag{3}$$

The derivative of U with respect to a gives the energy release rate

$$G = -\frac{\partial U}{\partial a} = \frac{E\delta^2}{144(1-\nu^2)\pi w} g_1(\tilde{a}) \tag{4}$$

with $g_1(\tilde{a}) = f(\tilde{a})/g_0^2(\tilde{a})$. Substituting Equation (4) into (3) gives

$$U = w \cdot g(\tilde{a}) \cdot G \tag{5}$$

where $g(\tilde{a}) = g_0(\tilde{a})/f(\tilde{a})$.

The energy release rate increases with δ. When the critical value, G_{cr}, is reached, the crack will overcome the fiber array and jump forward, leaving the fibers that bridge behind across the fracture flanks. Eventually, the fibers

will be broken apart or pulled out. The crack will keep advancing until the crack growth driving force is balanced by the fracture resistance, as depicted in Figure 1(b). During the crack jump, the deflection δ_{cr} can be assumed constant. At the onset of the crack jump, according to Equation (4)

$$G_{cr} = \frac{E\delta_{cr}^2}{144(1-\nu^2)\pi w} g_1(\tilde{a}_0) \tag{6}$$

where $\tilde{a}_0 = a_0/w$, with a_0 being the initial crack length. If the crack jump length Δa is smaller than a_0, based on experimental observations of dynamic cracking, the critical energy release rate to arrest the advancing crack is nearly the same as the quasi-static fracture resistance (Hellan, 1994). Thus, immediate after the crack jump,

$$G_{cm} = \frac{E\delta_{cr}^2}{144(1-\nu^2)\pi w} g_1(\tilde{a}_1) \tag{7}$$

where G_{cm} is the fracture resistance of cement matrix, $\tilde{a}_1 = a_1/w$, and $a_1 = a_0 + \Delta a$ is the crack length after the crack jump. Combination of Equations (6) and (7) leads to

$$\Delta\tilde{a} = \frac{\Delta a}{w} = f_1(\tilde{G}) \tag{8}$$

where $\tilde{G} = G_{cr}/G_{cm}$, and f_1 is a function reflecting the relationship between the crack jump length and the fracture toughness.

Through Equation (5), the decrease in strain energy stored in the beam can be obtained as

$$\Delta U = U_0 - U_1 = wg(\tilde{a}_0)G_{cr} - wg(\tilde{a}_1)G_{cm} \tag{9}$$

where U_0 and U_1 are the strain energies before and after the crack jump, respectively. The value of ΔU should be equal to the fracture work, i.e.

$$\Delta U = G_{cm}\Delta a + W_f \tag{10}$$

where W_f is the work associated with the failure of fibers per unit thickness. Substitution of Equations (8) and (9) into (10) gives

$$g(\tilde{a}_0)\tilde{G} - g[\tilde{a}_0 + f_1(\tilde{G})] - f_1(\tilde{G}) = \tilde{W} \tag{11}$$

where $\tilde{W} = W_f/(G_{cm}w)$. It can be seen that the toughening effect of the regular fiber array, $\tilde{G}$, is determined by a single parameter $\tilde{W}$, collecting

together the factors of fibers and matrix. Note that, since $W_f \geq 0$, $\tilde{W} \geq 0$ and $\tilde{G} \geq 1$, as they should be.

TOUGHENING EFFECTS OF A FIELD OF FIBERS

In a real FRC, the fibers are usually dispersed in the cementitious matrix nearly homogeneously, and therefore there are a field of fibers ahead of the crack tip. When $G = G_{cr}$, the crack front can break through the first fiber array. However, usually before the energy release rate can decrease to G_{cm} the front will encounter the next array and be arrested there. To keep the crack front advancing, in addition to G_{cr}, extra 'driving force' is required to overcome the resistance of the multiple fiber arrays.

At the steady state, the fracture work caused by the field of fibers, G_B, can be studied in the framework of the classic Anderson–Bergkvist model (Anderson and Bergkvist, 1970)

$$G_B = NW_{f0} \tag{12}$$

where $N = 1/D^2$ is the number of fibers exposed in unit area of fracture surface, D is the average distance between adjacent fibers, and $W_{f0} = W_f D$ is the fracture work of a single fiber. Thus, the overall critical energy release rate, G_{RFC}, can be stated as

$$\tilde{G}_{FRC} = \tilde{G} + \tilde{G}_B = \tilde{G} + \chi\tilde{W} \tag{13}$$

where $\tilde{G}_{RFC} = G_{RFC}/G_{cm}$, $\tilde{G}_B = G_B/G_{cm}$, and $\chi = w/D$.

If the fibers are broken apart, $W_{f0} = G_f(\pi r^2)$, with G_f being the effective fracture resistance of the polymer material and r being the cross-sectional radius. Usually the fiber content is measured by the fiber volume fraction, c, which, for uniformly dispersed fibers, can be related to D as

$$c = \frac{\pi r^2 (2r\rho)}{D^3} \tag{14}$$

where $\rho = l_f/(2r)$ is the fiber aspect ratio and l_f is the fiber length. Consequently, the parameter $\tilde{W}$ can be rewritten as

$$\tilde{W} = \frac{\pi}{(2\pi)^{1/3}} \frac{r}{w} \left(\frac{c}{\rho}\right)^{1/3} \tilde{G}_f \tag{15}$$

where $\tilde{G}_f = G_f/G_{cm}$. Similarly, we have $\chi = (w/r)(c/2\pi\rho)^{1/3}$.

If the fiber length is shorter than a critical value, the fibers will be pulled out. Under this condition, $W_{f0} = k_{cm}(2\pi r)(l_f/2)^2/2$, where k_{cm} is the effective internal friction, and thus

$$\tilde{W} = \frac{\pi}{(2\pi)^{1/3}} \frac{k_{cm} r^2}{w G_{cm}} \rho^{5/3} c^{1/3} \tag{16}$$

DISCUSSION

Figure 2 shows the relationship between the fracture resistances and $\{\tilde{W}, \chi\}$. As $\tilde{W}$ rises, both G_{FRC} and G_{cr} increase, while χ affects only G_{FRC}. When ρ, c, k_{cm}, and r are small, or w and G_{cm} are large, the value of $\tilde{W}$ is close to 0 and the total fracture resistance is only slightly higher than G_{cm}. The contribution of the bridging effect, G_B, is negligible. If $\tilde{W}$ exceeds 0.02, G_{FRC} rises rapidly and the contributions from G_{cr} and G_B are comparable with each other. In engineering practice, the volume fraction of fibers is often below 1% and thus the toughening effect falls in this range. If $\tilde{W}$ keeps increasing, eventually G_B is dominant and the effect of post-cracking ductility is pronounced.

If the fiber aspect ratio is relatively high, the critical force required to break apart the fiber is lower than that required to pull it out, and therefore the value of $\tilde{W}$ should be calculated through Equation (15). Otherwise, Equation (16) should be used. Due to the strong polymer–cement bonding

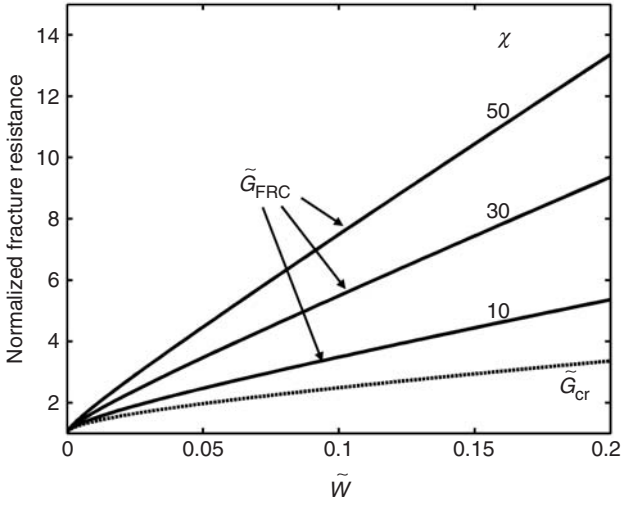

Figure 2. *The fracture resistance as a function of $\tilde{W}$ and χ.*

and interlocking, usually debonding does not take place at the fiber–matrix interface. Rather, the failure is triggered by the separation of the interface transition zone (ITZ). Thus, the value of k_{cm} should be around 1 MPa. As the fiber aspect ratio is small, through Equation (15), it can be seen that fiber breakage requires infinite large force as $\rho \to 0$, making it energetically unfavorable. Under this condition, increasing fiber aspect ratio has a beneficial effect to the fracture resistance.

The crack jump length across a regular fiber array can be obtained through Equation (8). In addition to $\tilde{W}$, Δa is also related to the initial crack length, a_0 (Figure 3), which has been well known in the area of dynamic fracture mechanics (Hellan, 1994). In homogeneous materials, the crack jump length should be proportional to the initial crack length. In fiber reinforced cements, however, the linearity is lost due to the heterogeneous nature of crack advance. In the range of $\tilde{G}$ under consideration, $\Delta a/a_0$ is smaller than 1, indicating that the above discussion is self-compatible.

According to Equations (15) and (16), In either fiber breakage or fiber pull-out mode, $\tilde{W}$ is related to a_0, so is the critical energy release rate; that is, G_{cr} is not a material constant. The longer the initial crack, the lower the fracture resistance, as shown in Figure 4. This phenomenon should be attributed to the nonuniform nature of the crack front advance. Since the fiber size and spacing do not vary with crack length, at the front of a longer crack the fibers look 'smaller' and thus the toughening effectiveness is lower. Note that this size effect is pronounced only for short cracks. When a_0 is much larger than the characteristic microstructure length, G_{cr} is insensitive to a_0.

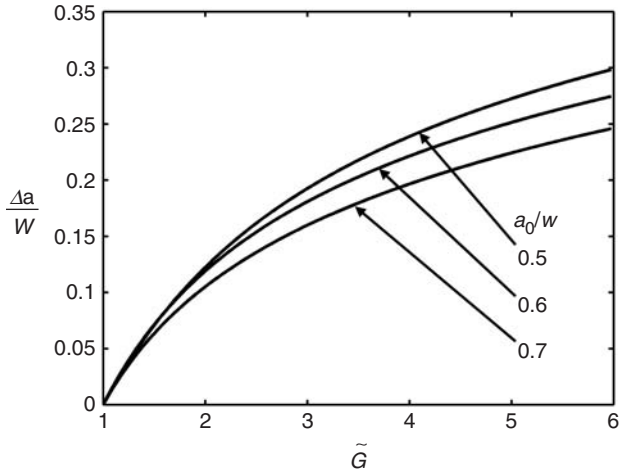

Figure 3. *The crack jump length as a function of $\tilde{G}$ and a_0/w.*

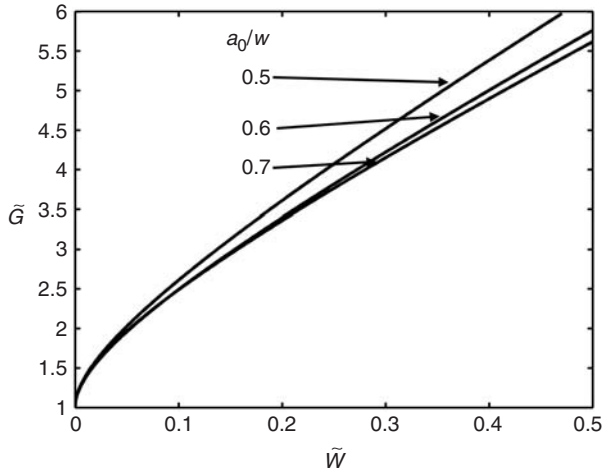

Figure 4. *The crack length dependence of G_{cr}.*

CONCLUSIONS

A simple model is developed based on energy analysis to evaluate the toughening effect of polymer fibers in cementitious materials. The toughening effect of a regular fiber array can be collectively described by a single parameter, $\tilde{W}$. The FRC toughness increases with the volume fraction and the toughness of fibers. With a constant fiber volume fraction, increasing fiber radius has a beneficial effect to the fracture toughness. When $\tilde{W}$ is relatively low, the contribution of bridging effect is negligible. As $\tilde{W}$ increases, post-cracking ductility becomes increasingly pronounced. There is an intrinsic size effect of G_{cr}, primarily due to the nonuniform nature of crack advance.

ACKNOWLEDGMENT

This work was supported by The National Science Foundation under Grant No. CMS-0408276.

REFERENCES

Anderson, H. and Bergkvist, H. (1970). Analysis of a Nonlinear Crack Model, *J. Mech. Phys. Solids*, **18**: 1–28.

Banthia, N. and Nandakumar, N. (2003). Crack Growth Resistance of Hybrid Fiber Reinforced Cement Composites, *Cem. Concr. Comp.*, **25**: 3–9.

Barbero, E.J., Greco, F. and Lonetti, P. (2005). Continuum Damage-healing Mechanics with Application to Self-healing Composites, *Inter. J. Damage Mech.*, **14**: 51–81.

Bayasi, Z. and Al Dhaheri, M. (2002). Effect of Exposure to Elevated Temperature on Polypropylene Fiber-Reinforced Concrete, *ACI Mater. J.*, **99**: 22–26.

Bayasi, Z. and McIntyre, M. (2002). Application of Fibrillated Polypropylene Fibers for Restraint of Plastic Shrinkage Cracking in Silica Fume Concrete, *ACI Mater. J.*, **99**: 337–344.

Chan, L.C., Cheng, C.H., Jie, M. and Chow, C.L. (2005). A Damage-coupled Criterion of Localized Necking Based on Acoustic Tensor, *Inter. J. Damage. Mech.*, **14**: 83–96.

Gross, B. and Srawley, J.E. (1972). Stress Intensity Factors for Bend and Compact Specimens, *Eng. Fract. Mech.*, **4**: 587–589.

Haj Ali, R. and El Hajjar, R. (2004). Mode-I fracture Toughness Testing of Thick Section FRP Composites using the ESE(T) Specimen, *Eng. Fract. Mech.*, **35**: 631–643.

Hellan, K. (1994). *Introduction to Fracture Mechanics*, McGraw-Hill, New York.

Ju, J.W., Ko, Y.F. and Ruan, H.N. (2006). Effective Elastoplastic Damage Mechanics for Fiber Reinforced Composites with Evolutionary Complete Fiber Debonding, *Inter. J. Damage Mech.*, **15**: 237–265.

Lee, S., Jeng, S.M. and Yang, J.M. (1995). Modeling and Simulation of the Effect of Fiber Breakage on Creep Behavior of Fiber-reinforced Metal Matrix Composites, *Mech. Mater.*, **21**: 303–312.

Kamada, T. and Li, V.C. (2000). The Effects of Surface Preparation on the Fracture Behavior of ECC/Concrete Repair System, *Cem. Concr. Compos.*, **22**: 423–431.

Kodur, V.K.R., Cheng, F.P., Wang, T.C. and Sultan, M.A. (2003). Effect of Strength and Fiber Reinforcement on the Fire Resistance of High Strength Concrete Columns, *J. Struct. Eng. ASCE*, **129**: 253–259.

Kullaa, J. (1994). Constitutive Modeling of Fiber-reinforced Concrete under Uniaxial Tensile Loading, *Compos.*, **25**: 935–944.

Mamlouk, M.S. and Zaniewski, J.P. (1999). *Materials for Civil and Construction Engineers*, Addison-Wesley, New York.

Mindess, S., Young, J.F. and Darwin, D. (2002). *Concrete*, Pearson Education, Upper Saddle River, NJ.

Mower, T.M. and Argon, A.S. (1995). Experimental Investigations of Crack Trapping in Brittle Heterogeneous Solids, *Mech. Mater.*, **19**: 343–364.

Ouaar, A., Doghri, I., Delannay, L. and Thimus, J.F. (2007). Micromechanics of the Deformation and Damage of Steel Fiber-reinforced Concrete, *Inter. J. Damage Mech.*, **16**: 227–260.

Qiao, Y. (2003). Fracture Toughness of Composite Materials Reinforced by Debondable Particulates, *Scripta Mater.*, **49**: 491–496.

Ulm, F.J. (2003). Chemomechanics of Concrete at Finer Scales, *Mater. Struct.*, **36**: 426–438.

Zollo, R.F. (1997). Fiber-reinforced Concrete: An Overview After 30 years of Development, *Cem. Concr. Compos.*, **19**: 107–122.

Zou, P.X.W. (2003). Flexural behavior and Deformability of Fiber Reinforced Polymer Prestressed Concrete Beams, *J. Compos. Constr.*, **7**: 275–284.